European Journal of Radiology Open 8 (2021) 100335

Contents lists available at ScienceDirect

European Journal of Radiology Open

journal homepage: www.elsevier.com/locate/ejro

Mitral annular disjunction in patients with severe aortic stenosis: Extent and reproducibility of measurements with computed tomography

T. Tsianaka [a], I. Matziris [b], A. Kobe [a], A. Euler [a], N. Kuzo [b], L. Erhart [b], S. Leschka [c], R. Manka [a,b,d], A.M. Kasel [b], F.C. Tanner [b], H. Alkadhi [a], M. Eberhard [a,*]

[a] Institute of Diagnostic and Interventional Radiology, University Hospital Zurich, University of Zurich, Switzerland
[b] Department of Cardiology, University Heart Center Zurich, Zurich, Switzerland
[c] Division of Radiology and Nuclear Medicine, Kantonsspital St.Gallen, Switzerland
[d] Institute for Biomedical Engineering, University and ETH Zurich, Zurich, Switzerland

ARTICLE INFO

Keywords:
Mitral annular disjunction
Mitral valve prolapse
Mitral valve
Computed tomography
Transcatheter aortic valve replacement

ABSTRACT

Objectives: To determine with CT the prevalence and extent of mitral annular disjunction (MAD) in patients undergoing transcatheter aortic valve replacement (TAVR) and its association with mitral valve disease and arrhythmia.

Methods: We retrospectively evaluated 408 patients (median age, 82 years; 186 females) with severe aortic stenosis undergoing ECG-gated cardiac CT with end-systolic data acquisition. Baseline and follow-up data were collected in the context of a national registry. Two blinded, independent observers evaluated the presence of MAD on multi-planar reformations. Maximum MAD distance (left atrial wall-mitral leaflet junction to left ventricular myocardium) and circumferential extent of MAD were assessed on CT using dedicated post-processing software. Associated mitral valve disease was determined with echocardiography.

Results: 7.8 % (32/408) of patients with severe aortic stenosis had MAD. The maximum MAD was 3.5 mm (interquartile range: 3.0–4.0 mm). The circumferential extent of MAD comprised 34 ± 15 % of the posterior and 26 ± 12 % of the entire mitral annulus. Intra- and interobserver agreement for the detection of MAD on CT were excellent (kappa: 0.90 ± 0.02 and 0.92 ± 0.02). Mitral regurgitation (p = 1.00) and severe mitral annular calcification (p = 0.29) were similarly prevalent in MAD and non-MAD patients. Significantly more patients with MAD (6/32; 19 %) had mitral valve prolapse compared to those without (6/376; 2 %; $p < 0.001$). MAD was not associated with arrhythmia before and after TAVR ($p > 0.05$).

Conclusions: Using CT, MAD was found in 7.8 % of patients with severe aortic stenosis, with a higher prevalence in patients with mitral valve prolapse. We found no association of MAD with arrhythmia before or after TAVR.

1. Introduction

Mitral annulus disjunction (MAD) was first described in 1981 in a patient with mitral valve prolapse and sudden cardiac death [1]. It refers to an anatomic variation with spatial displacement of the left atrial wall-mitral leaflet junction and left ventricular wall during systole [1,2]. The disjunctive annulus is functionally decoupled from the left ventricle leading to paradoxical annular dynamics with systolic expansion and flattening [3]. MAD has been related to mitral valve prolapse and myxomatous mitral valve disease [3–6] and may be associated with an increased risk for ventricular arrhythmia [7]. Recently, Chivulescu et al. showed that MAD is highly prevalent in patients with Marfan and Loeys–Dietz syndromes and associated with adverse outcomes, including aortic events at a younger age and the need for mitral valve surgery [8].

Echocardiography, being the most widely used cardiac imaging modality, enables the detection of MAD [5,9]. However, particularly retrospective assessment of MAD with echocardiography may be hampered by reduced image quality, atrial fibrillation, and in patients with posterior myocardial infarction [9]. This is reflected by the results

Abbreviations: CT, computed tomography; ECG, electrocardiogram; IQR, inter-quartile range; MADmitral, annular disjunction; MR, mitral regurgitation; TAVR, transcatheter aortic valve replacement.

* Corresponding author at: Institute of Diagnostic and Interventional Radiology, University Hospital Zurich, Raemistrasse 100, CH-8091, Zurich, Switzerland.
E-mail address: matthias.eberhard@usz.ch (M. Eberhard).

https://doi.org/10.1016/j.ejro.2021.100335
Received 22 January 2021; Received in revised form 25 February 2021; Accepted 1 March 2021

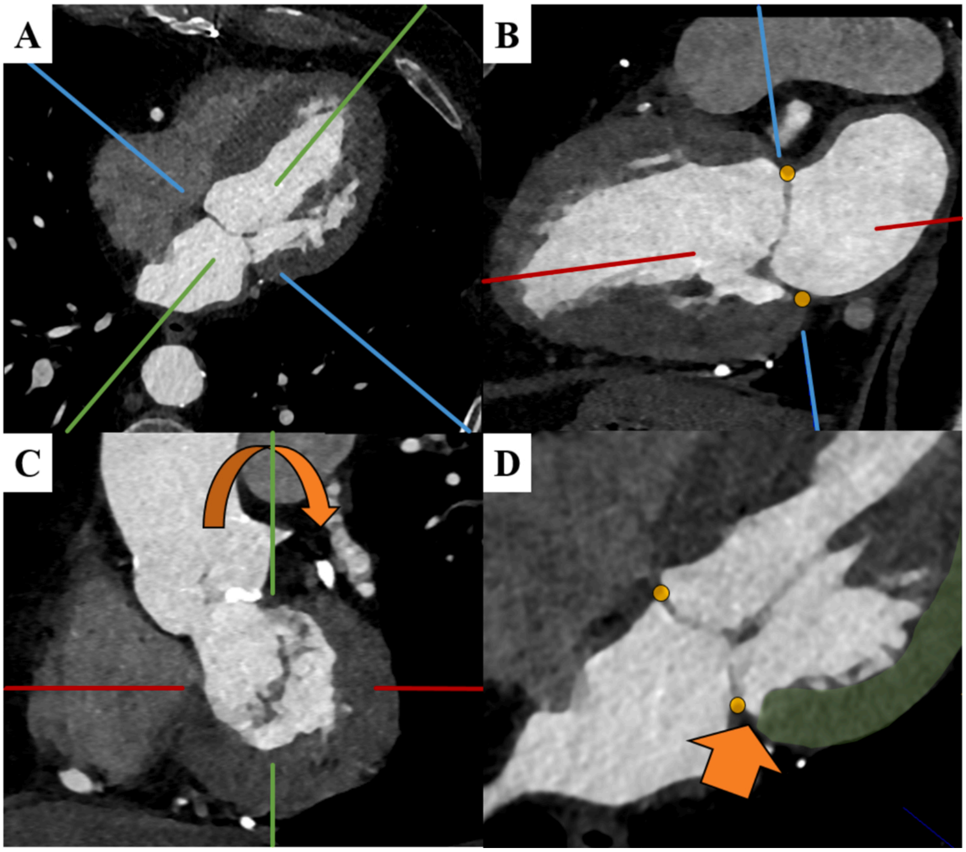

Fig. 1. CT assessment of mitral annular disjunction (MAD).
The MAD assessment starts on the axial plane (A). To derive the vertical long axis (VLA) view the crosshairs are adjusted to pass through the center of the mitral valve and left ventricular apex. On the VLA (B), crosshairs are adjusted to align with the left atrial wall- mitral leaflet junction (yellow markers). On the acquired short-axis view on a plane through the mitral valve (C), crosshairs are rotated to assess the corresponding long axis image (D) for the presence of MAD (orange arrow). MAD is defined as spatial displacement of the left atrial wall-mitral leaflet junction (yellow marker) and the left ventricular wall (green) during systole (For interpretation of the references to colour in this figure legend, the reader is referred to the web version of this article.).

from the study by Konda et al. who had to exclude 34 % of the 2188 consecutive patients referred to echocardiography in their retrospective analysis of MAD because of limitations in image quality [9].

Cardiac computed tomography (CT) represents a widely used imaging modality for the evaluation of structural heart disease. This is mainly due to its non-invasiveness and its high spatial resolution providing isotropic voxels enabling the reconstruction of images of the heart with equal quality in any arbitrary plane [10–14]. Specifically, CT allows for an assessment of the mitral valve apparatus including the leaflet/annulus complex with high accuracy [14–17]. In patients with aortic stenosis undergoing transcatheter aortic valve replacement (TAVR) relevant mitral valve disease frequently coexists in around one third of patients [18,19].

The purpose of our study was *i*) to evaluate the feasibility of CT to detect and measure MAD, *ii*) to determine the prevalence and extent of MAD in TAVR patients, *iii*) to assess the association of MAD with mitral valve disease, and *iv*) to assess the association of MAD with arrhythmia before and after TAVR implantation.

2. Material and methods

2.1. Patient population

Baseline data collection was performed in the context of a nationwide prospective registry (SWISS TAVI registry). This study had local institutional and ethics committee approval. All patients provided written informed consent.

Between November 2008 and May 2019, we retrospectively evaluated 408 patients (median age, 82 years; 186 females) with severe aortic stenosis. All patients underwent CT, triggered in end-systole, as part of the institutional pre-procedural protocol prior to transcatheter aortic valve replacement (TAVR). Patient demographics, cardiovascular risk factors and medical history were noted for each patient. Arrhythmia before and after TAVR as well as new onset arrhythmia including the need for pacemaker implantation within 30-days after the intervention were recorded [20].

2.2. CT data acquisition and image reconstruction

All patients underwent CT on either a second- or third-generation dual-source CT scanner (SOMATOM Force; SOMATOM Definition Flash; Siemens Healthineers, Forchheim, Germany). Prospectively ECG-gated high-pitch CT angiography of the thoracoabdominal aorta was performed with our scanner-specific protocols.

Using the second-generation dual-source CT scanner we applied the following scan and reconstruction parameters [21]: tube voltage, 100kVp; tube current, automated attenuation-based tube current modulation was used with a reference tube current-time product of 320 mAs/rotation; pitch, 3.2; gantry rotation time, 0.25 s; collimation, 128 × 0.6 mm; slice thickness of 0.6 mm, an increment of 0.5 mm and a soft tissue convolution kernel (B30f) with Sinogram Affirmed Iterative Reconstruction (SAFIRE, Siemens Healthineers, Forchheim, Germany) at strength level 3. The contrast media protocol was as follows: First, 45 mL Iopromide (Ultravist 370; Bayer Vital, Leverkusen, Germany) at a flow rate of 5 mL/s was intravenously injected, directly followed by 35 mL of a second bolus of Iopromide and with a 60-mL bolus of saline chaser, both at the flow rate of 2.5 mL/s.

Using the third-generation dual-source CT we applied the following scan and reconstruction parameters [22]: tube voltage, automatic tube voltage selection; automatic attenuation-based tube current modulation; section acquisition, 2.0 × 192.0 × 0.6 mm with the z-flying focal spot; pitch, 3.2; and gantry rotation time, 250 msec, slice thickness, 0.6 mm, an increment of 0.4 mm and a soft-tissue kernel (Bv36) with advanced modeled iterative reconstruction (ADMIRE; Siemens Healthineers, Forchheim, Germany) at strength level 4. The contrast media protocol was as follows: Undiluted Iopromide (Ultravist 370; Bayer Vital, Leverkusen,

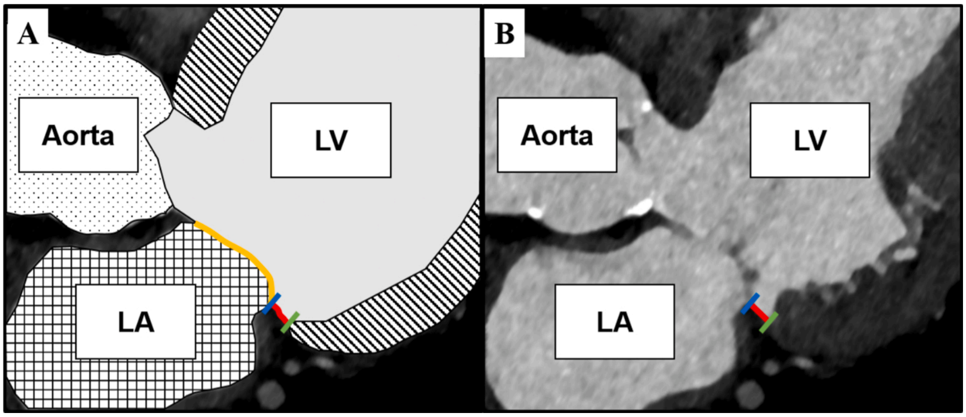

Fig. 2. Measurement of the mitral annulus disjunction (MAD) length.
Panel A schematically illustrates the spatial disjunction (red line) of the basal inferolateral left ventricular myocardium (green) and the left atrial wall-mitral leaflet junction (blue) assessed on a 3-chamber view. The mitral valve is shown in yellow. Panel B shows the MAD length measurement (red line) on the corresponding CT image.
Abbreviations: LA, left atrium; LV, left ventricle (For interpretation of the references to colour in this figure legend, the reader is referred to the web version of this article.).

Germany) was injected into an antecubital vein. Contrast media volume and flow rate were adapted depending on the proposed tube voltage (as detailed in [22]). Contrast media injection was followed by injection of a 50-mL saline bolus at a rate of 4 mL/sec. For both scanners, bolus tracking was performed in the ascending aorta with a signal attenuation threshold of 100 Hounsfield units at a tube voltage of 120 kV.

Aortic root structures undergo significant dimensional changes throughout the cardiac cycle [23]. Therefore, it is recommended to measure the aortic annulus size in end-systole to avoid undersizing of TAVR prosthesis [10]. Due to the contraction of the left ventricular myocardium, MAD can be assessed during systole. Maximum MAD measurements are recommended to be performed in end-systole [9,24].

The CT scan was started automatically based on the previous 10 heartbeats in order to reach the 30 % RR-interval at the level of the sinutubular junction. Scanning ranged from the lung apex to the lesser trochanter of the femur. Cardiac CT images were reconstructed with 0.6 mm section thickness and a 0.4 mm increment.

2.3. CT assessment of MAD

One observer (T.T., 5 years of experience in cardiovascular imaging) evaluated the presence or absence of MAD using a dedicated post-processing software (Cardiac function application, Siemens syngo.via, version VB30A, Siemens Healthineers, Forchheim, Germany). The presence of MAD was evaluated on multi-planar reformations (Fig. 1). The length of the MAD was measured from the left atrial wall-posterior mitral leaflet junction to the top of the left ventricular wall during end-systole (Fig. 2) [24]. The maximum distance as well as the distance in each dedicated left ventricular long axis view (2-, 3-, and 4-chamber left ventricular long-axis) were recorded. To assess interobserver and intraobserver variability, 300 randomly selected cases were re-evaluated by observer one (T.T.) after 2 months to avoid recall bias and by a second reader (A.K., 5 years of experience in cardiovascular imaging), both blinded to the initial results.

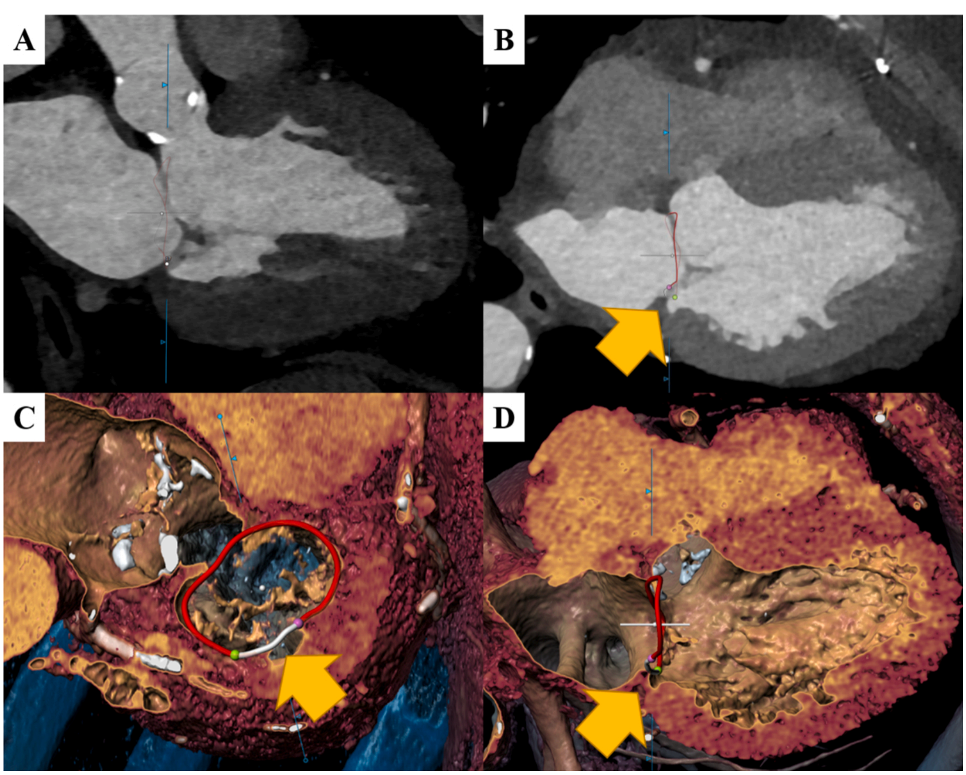

Fig. 3. Extent of mitral annular disjunction (MAD).
Panels A–D illustrates measurements of the extent and proportion of the mitral annulus involved in MAD. After placing 16 seed points along the mitral annulus (in the long axis reformation, A), the circumference of the mitral annulus is determined semi-automatically by the software (B). The extent of the mitral annulus displaced from the left ventricular myocardium (B) was marked with the green and purple seed point (C) and the proportion of the annulus circumference with MAD is shown in white (C and D). The MAD extent was recorded and used to calculate the ratio of the MAD extent divided by the entire and the posterior mitral annular circumference (For interpretation of the references to colour in this figure legend, the reader is referred to the web version of this article.).

2.4. CT assessment of the mitral annulus

In all patients with MAD, we additionally evaluated the mitral annular dimensions using an advanced visualization, segmentation and image analysis software (3mensio Structural Heart 8.1, Pie Medical Imaging, Maastricht, NL). After independently placing 16 seed points along the mitral annulus (in the long axis reformation), the circumference of the mitral annulus both in 3D and 2D (including the anterior and posterior part), the mitral annular area, the intercommissural distance and the septolateral distance were semiautomatically determined by the software [25]. The proportion of the mitral annulus displaced from the left ventricular myocardium was recorded and used to calculate the circumferential involvement of the MAD in regard to the posterior mitral annulus and the entire mitral annulus (Fig. 3). Severe mitral annular calcification was defined as calcification of ≥ ½ of the mitral annular circumference [26].

2.5. Echocardiography

The degree of mitral regurgitation (MR) was assessed using structural, spectral, and color-Doppler images and were graded as mild, moderate, or severe using multi-parametric assessments according to the European Association of Cardiovascular Imaging/American Society of Echocardiography recommendations [27,28].

Mitral valve prolapse was assessed in the parasternal long-axis view as systolic displacement of the mitral leaflet into the LA of at least 2 mm from the mitral annular plane, according to the American Society of Echocardiography guidelines [29] and according to European Association of Cardiovascular Imaging recommendations, which defines mitral valve prolapse as abnormal systolic displacement of mitral valve coaptation point into the left atrium below the annular plane [28]. As the echocardiographic examinations had been performed without focusing specifically on detecting MAD, we did not include an echocardiographic MAD assessment as these results might have underestimated the MAD prevalence.

2.6. Statistical analysis

Parametric and non-parametric distributed, continuous variables are presented as mean and standard deviation or medians and inter-quartile ranges (IQR), respectively. Categorical variables are presented as numbers and percentages. Pairwise comparison was performed using student's *t*-test or the Mann-Whitney U-test, where appropriate. Categorical variables were using the Pearson's Chi-square or Fisher's exact test, where appropriate. Intra- and interobserver agreement to detect MAD was calculated using Cohen's kappa. Bland-Altman analysis was applied to evaluate the reproducibility for MAD maximum measurements between and within observers.

A two-sided p-value of 0.05 was considered statistically significant. All analyses were performed with SPSS for Windows 25.0 (Chicago, IL, USA).

3. Results

3.1. Baseline characteristics and prevalence of MAD

Table 1 summarizes the patient demographics. From the 408 patients with severe aortic stenosis, 32 (7.8 %) showed MAD on CT. Median patient heart rate was 70/min (minimum, 48/min; maximum, 130/min). A representative example is shown in Fig. 4. MAD and non-MAD patients did not show significant differences in baseline characteristics (see Table 1).

3.2. CT measurements

CT measurements in MAD patients are shown as Table 2. Patients with MAD had a median posterior mitral annular circumference of 94.6 ± 14.7 mm and a median overall mitral annular circumference of 125.6 ± 16.9 mm. The median circumferential extent of the MAD was 32.9 ± 17.1 mm, comprising 34 ± 15 % of the posterior mitral annular circumference and 26 ± 12 % of the entire mitral annular circumference.

The median maximum MAD distance from the LV free wall was 3.5 mm (IQR: 3.0–4.0 mm). In 21 of the 32 patients (65 %), the maximum MAD distance was found inferior in the 2-chamber left ventricular long-axis view.

Table 1
Baseline demographics.

	OVERALL n = 408 Median (Interquartile Range)	WITHOUT MAD n = 376 Median (Interquartile Range)	WITH MAD n = 32 Median (Interquartile Range)	p-value
Age (years)	82 (78–85)	82 (78–85)	82 (78–87)	0.76
Body mass index (kg/m^2)	26.4 (23.9–29.7)	26.4 (23.9–29.9)	24.8 (23.6–28.3)	0.14
Body surface area (m^2)	1.81 (1.7–1.99)	1.81 (1.70–1.97)	1.83 (1.65–2.00)	0.81
EuroSCORE II	4.0 (2.3–8.0)	4.2 (2.3–8.1)	3.0 (2.0–5.0)	0.056
	Mean (Standard deviation)	**Mean (Standard deviation)**	**Mean (Standard deviation)**	**p-value**
Weight (kg)	74 (±14)	74 (±14)	73 (±15)	0.65
Height (cm)	165 (±9)	165 (±10)	167 (±9)	0.30
	Count (Percentage)	**Count (Percentage)**	**Count (Percentage)**	**p-value**
Females	192 (47 %)	176 (47 %)	16 (50 %)	0.85
NYHA III or IV	156 (38 %)	141 (38 %)	15 (47 %)	0.34
Arterial hypertension	337 (83 %)	309 (82 %)	28 (88 %)	0.63
Diabetes	109 (27 %)	101 (27 %)	8 (25 %)	1.0
Current/Previous smokers	165 (40 %)	150 (40 %)	15 (47 %)	0.46
Dyslipidaemia	274 (67 %)	248 (66 %)	26 (81 %)	0.081
Chronic obstructive pulmonary disease	63 (15 %)	59 (16 %)	4 (13 %)	0.80
Clinically relevant coronary artery disease	230 (56 %)	215 (57 %)	15 (47 %)	0.27
Previous cardiovascular interventions	98 (24 %)	87 (23 %)	11 (34 %)	0.19
Cerebrovascular disease	80 (20 %)	87 (23 %)	3 (9 %)	0.17
Peripheral artery disease	86 (21 %)	79 (21 %)	7 (22 %)	1.0
Moderate/ severe mitral regurgitation	107 (26 %)	99 (26 %)	8 (25 %)	1.0
Severe mitral annular calcification	100 (25 %)	85 (24 %)	15 (27 %)	0.29
Mitral valve prolapse	12 (3 %)	6 (2 %)	6 (19 %)	**<0.001**

Abbreviations: EuroSCORE, European System for Cardiac Operative Risk Evaluation; NYHA, New York Heart Association.

3.3. Agreement between observers

Intra- and interobserver reproducibility for MAD assessment with CT showed excellent agreement with kappa values of 0.90 ± 0.02 and 0.92 ± 0.02, respectively. Repeated measurements of the maximum MAD distance from the LV free wall resulted in a mean difference of 0.1 ± 1.1 mm within and 0.0 ± 0.8 mm between observers (Fig. 5).

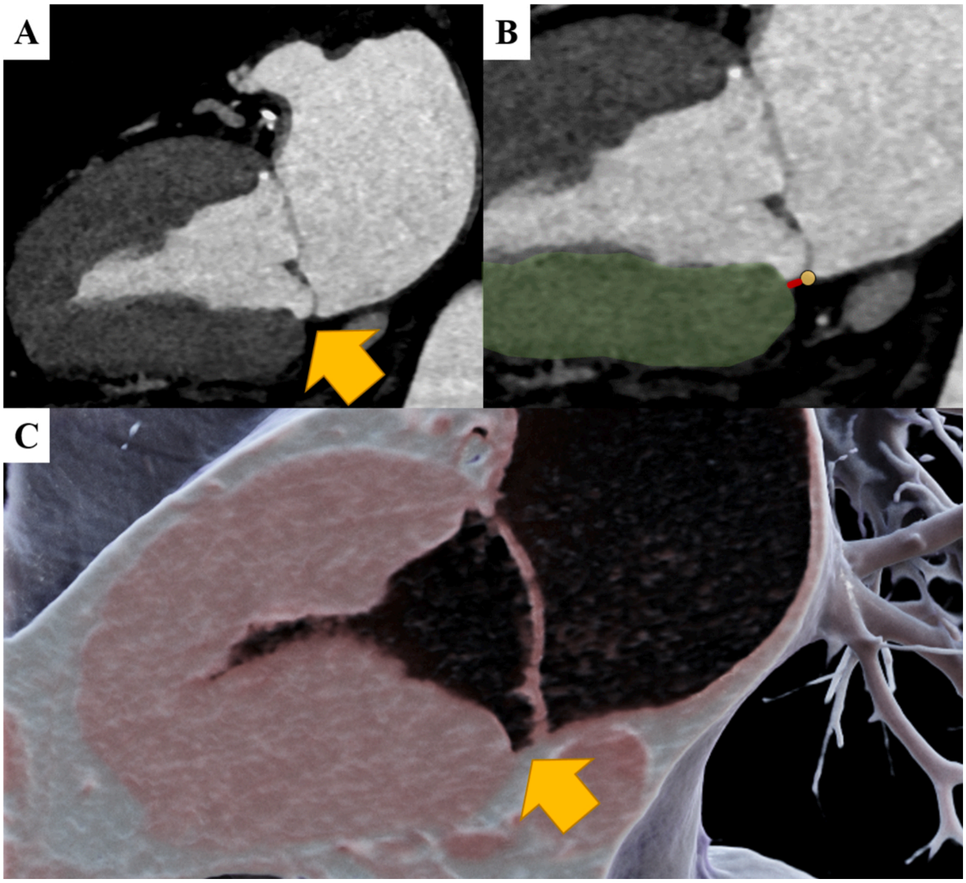

Fig. 4. Representative case example.
Representative case of a 66-year-old male patient with Mitral annular disjunction (MAD). MAD (yellow arrow) is shown in the 2-chamber view (A). MAD length measurement (B) was performed between the left ventricular myocardium (green) and the left atrial wall-mitral leaflet junction (yellow marker). Panel C illustrates the MAD using 3D cinematic rendering (For interpretation of the references to colour in this figure legend, the reader is referred to the web version of this article.).

Table 2
CT measurements in patients with mitral annular disjunction (MAD).

	Median (IQR)
MAD maximum distance (mm)	3.5 (3.0–4.0)
MAD 2CH distance (mm)	3.5 (3.0–4.0)
MAD 3CH distance (mm)	2.5 (1.4–3.3)
MAD 4CH distance (mm)	2.2 (1.3–3.0)
	Mean (Standard Deviation)
Mitral Annular Area (cm^2)	10.9 (± 3.2)
Mitral Annular Perimeter (mm)	125.6 (± 16.9)
Anterior Annular Perimeter (mm)	31.0 (± 4.3)
Posterior Annular Perimeter (mm)	94.6 (± 14.7)
Mitral Annular Disjunction Perimeter (mm)	32.9 (± 17.1)
Anteroposterior distance (mm)	28.9 (± 5.4)
Trigone-to-trigone distance (mm)	28.4 (± 4.1)

Abbreviations: 2CH, left ventricular long-axis 2-chamber view; 3CH, left ventricular long-axis 3-chamber view; 4CH, left ventricular long-axis 4-chamber view; MAD, mitral annular disjunction.

3.4. Association with mitral valve disease and mitral annular calcification

Moderate or severe MR was found in 107/408 patients (26 %). Severe mitral annular calcification was found in 100/408 patients (25 %). There were no significant differences for moderate/severe MR ($p = 1.00$) and severe mitral annular calcification ($p = 0.29$) between patients with and those without MAD. Six of the 32 patients (19 %) with MAD showed mitral valve prolapse, with a significantly higher prevalence in patients with as compared to those without MAD (6/376 patients, 1.6 %; $p < 0.001$).

3.5. Association with arrhythmia before and within 30-days after TAVR

There were no significant differences in atrial fibrillation/flutter, bundle branch or atrioventricular block in patients with compared to those without MAD before and after TAVR (all, $p > 0.05$, Table 3). Similarly, there was no significant difference in the need for pacemaker implantation before and within 30-days after TAVR between patients with and those without MAD (all, $p > 0.05$, Table 3).

4. Discussion

Our study shows that it is feasible to detect and evaluate MAD on CT. We could show that MAD was frequently (7.8 %) found in patients with severe aortic stenosis planned to undergo TAVR. In these patients, CT enabled a highly reproducible assessment of MAD with excellent intra- and interobserver agreement and small errors. The presence of MAD was not associated with a higher prevalence of moderate/severe MR or severe mitral annular calcification. However, patients with MAD significantly more often had associated mitral valve prolapse, being present in 19 % of these patients. In our study population, MAD was not associated with arrhythmia including the need for pacemaker implantation within 30-days after TAVR.

The prevalence of MAD in patients undergoing routine echocardiography referred for a variety of reasons is approximately 9 % with a mean maximum distance of 3.5 mm [9]. Interestingly, Konda et al. found that MAD was more frequent in patients with an otherwise “normal echocardiographic study” than in patients with specific cardiac diseases except for mitral valve prolapse [9]. Our patients showed a comparable prevalence (7.8 %) and similar extent of MAD with a maximum distance of 3.5 mm, comprising 34 % of the posterior mitral annular circumference and 26 % of the overall mitral annular circumference. Dejgaard et al. reported a median circumferential MAD extent

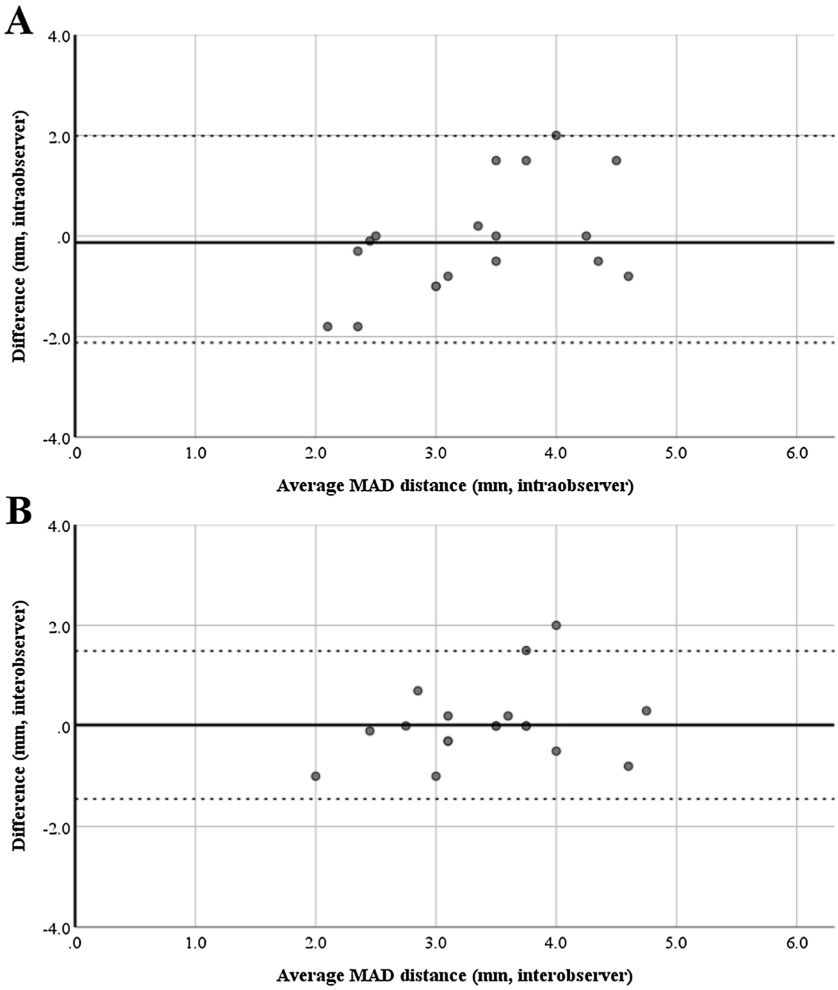

Fig. 5. Intra- and interobserver reproducibility of MAD distance measurements.
Bland-Altman plots illustrating narrow limits of agreement for intraobserver (Panel A, difference: 0.13 ± 1.08) and interobserver (Panel B, difference: 0.02 ± 0.75) variability of mitral annular disjunction (MAD) distance measurements.

Table 3
Arrhythmia before and after transcatheter aortic valve replacement (TAVR).

Before TAVR		without MAD n = 376	with MAD n = 32	p-value
Pacemaker		21 (6 %)	0 (0 %)	0.39
Type of arrhythmia	**Atrial fibrillation or flutter**	75 (21 %)	11 (34 %)	0.12
	Bundle branch block	91 (26 %)	4 (13 %)	0.13
	Atrioventricular block	60 (17 %)	6 (19 %)	0.81
After TAVR		without MAD n = 355	with MAD n = 32	p-value
Permanent pacemaker implantation within 30 days		66 (19 %)	4 (13 %)	0.48
Type of arrhythmia	**Atrial fibrillation or flutter**	58 (20 %)	8 (29 %)	0.33
	Bundle branch block	125 (43 %)	12 (43 %)	1.00
	Atrioventricular block	60 (21 %)	7 (25 %)	0.63

Cardiac rhythm was assessed in patients without permanent pacemakers only.
Abbreviations: TAVR, transcatheter aortic valve replacement.

of 150° in their cardiac magnetic resonance study of preselected patients with echocardiography-proven MAD [7]. However, the comparability is limited as Dejgaard et al. did not use a 3D volume data to measure the circumferential but acquired 6 left ventricle long-axis cine sequences with an interslice rotation of 30° [7]. Using 3D echocardiography, Lee et al. reported a circumferential mean extent of 87° in a cohort with a predominance of patients with mitral valve prolapse (comprising 2/3 of the study population) thus showing a similar circumferential extent as in our study [3].

MAD assessment is usually reported with echocardiography [3–6,9]. Recently, also cardiac magnetic resonance imaging was applied for the evaluation of MAD [7,30]. Both modalities are well suited for MAD assessment owing to their capability to visualize the mitral annular and left ventricular myocardial dynamics. CT provides high spatial resolution, three-dimensional volumetric data for the evaluation of the mitral annulus and adjacent structures [14,25]. Putnam et al. recently reported MAD in patients with severe MR and mitral valve prolapse undergoing cardiac CT for preoperative planning of mitral valve repair [24]. Our data adds to this study that MAD can be diagnosed not only in retrospectively ECG-gated cardiac CT data with reconstruction of all phases throughout the R-R interval [24], but also on a prospectively triggered high-pitch CT angiography study acquired at end-systole. Of course, the latter technique may underestimate the extent of MAD as the spatial displacement of the left atrial wall-mitral leaflet junction and left ventricular myocardium is assessable only at a single time-point during systole. Retrospective CT scanning may allow for the assessment of the true MAD size but has the disadvantage of a higher radiation dose. Regarding reproducibility, all non-invasive imaging modalities described above show similar excellent reproducibility for MAD assessment and measurements [4,5,9,24], similar to the results from our study.

New-onset arrhythmia is frequent in patients after TAVR and represents a major determinant of post-procedural morbidity and mortality [31,32]. In our patients, MAD was not associated with a higher prevalence of arrythmia both before and within 30-days after TAVR. One possible reason for this finding might be that MAD usually is more associated with ventricular but not with supraventricular arrhythmia or bradyarrhythmia [2]. The latter being more prevalent in patients after TAVR [31,32].

Dynamically, normal and nondisjunctive annulus contract in a saddle shape during systole [15]. In patients with a poor left ventricular function and functional mitral regurgitation, the mitral annulus is dilated and relatively adynamic [3]. In contrast, disjunctive annulus show a paradoxical systolic expansion and flattening, even in patients with preserved left ventricular function, indicating a functional decoupling from the ventricle [3]. Severe aortic stenosis and severe mitral regurgitation frequently coexists [18,19]. Whether mitral valve disease is independently associated with worse outcomes after TAVR remains a matter of debate [33]. Evidence-based recommendations and therapeutic strategies for concomitant severe aortic stenosis and mitral valve disease including surgical and transcatheter replacement and repair are still lacking due to insufficient data [28]. In these cases, knowledge of MAD and its association with mitral valve prolapse and mitral valve disease [2,8,24] could be helpful for planning surgical and transcatheter therapies. Moreover, further studies should assess whether the presence of MAD affects improvement of mitral valve function after patients with concomitant aortic stenosis and mitral valve regurgitation underwent TAVR.

Several study limitations merit consideration. First, this was a retrospective, single-center study, and our study included patients with severe aortic stenosis planned to undergo TAVR. This limits the generalizability of our results to a different patient population. Second, we did not compare MAD measurements from CT with those from echocardiography, as the latter were not performed focusing specifically on MAD. Finally, we did not evaluate potential associations of MAD with arrythmia in the long term (but only within 30 days).

5. Conclusion

In conclusion, our study shows that CT is feasible to detect and quantify MAD with high reproducibility. 7.8 % of patients with severe aortic stenosis show MAD on CT, with a maximum MAD of 3.5 mm, comprising 34 % of the posterior mitral annular circumference and 26 % of the overall mitral annular circumference. MAD was more frequently associated with mitral valve prolapse being present in 19 % of patients with MAD. We found no association of MAD with arrythmia before and within 30-days of the TAVR procedure.

Ethics statement

This retrospective study was approved by the local Ethics Committee and conducted according to the principles of the Declaration of Helsinki. Consent was obtained from all study subject

Source of funding

This research did not receive any specific grant from funding agencies in the public, commercial, or not-for-profit sectors.

CRediT authorship contribution statement

T. Tsianaka: Conceptualization, Data curation, Investigation, Methodology, Software, Visualization, Writing - original draft, Writing - review & editing. **I. Matziris:** Data curation, Investigation, Visualization, Writing - original draft, Writing - review & editing. **A. Kobe:** Data curation, Investigation, Visualization, Writing - original draft, Writing - review & editing. **A. Euler:** Conceptualization, Investigation, Methodology, Supervision, Validation, Writing - original draft, Writing - review & editing. **N. Kuzo:** Data curation, Investigation, Writing - original draft, Writing - review & editing. **L. Erhart:** Data curation, Investigation, Writing - original draft, Writing - review & editing. **S. Leschka:** Writing - original draft, Writing - review & editing. **R. Manka:** Conceptualization, Writing - original draft, Writing - review & editing. **A.M. Kasel:** Data curation, Investigation, Writing - original draft, Writing - review & editing. **F.C. Tanner:** Data curation, Investigation, Resources, Writing - original draft, Writing - review & editing. **H. Alkadhi:** Conceptualization, Investigation, Methodology, Project administration, Resources, Software, Supervision, Validation, Writing - original draft, Writing - review & editing. **M. Eberhard:** Conceptualization, Data curation, Formal analysis, Investigation, Methodology, Software, Supervision, Validation, Visualization, Writing - original draft, Writing - review & editing.

Declaration of Competing Interest

The authors report no declarations of interest.

Acknowledgements

None.

References

[1] S. Bharati, A.S. Granston, P.R. Liebson, H.S. Loeb, K.M. Rosen, M. Lev, The conduction system in mitral valve prolapse syndrome with sudden death, Am. Heart J. 101 (5) (1981) 667–670.

[2] C. Basso, S. Iliceto, G. Thiene, M. Perazzolo Marra, Mitral valve prolapse, ventricular arrhythmias, and sudden death, Circulation 140 (11) (2019) 952–964.

[3] A.P. Lee, C.N. Jin, Y. Fan, R.H.L. Wong, M.J. Underwood, S. Wan, Functional implication of mitral annular disjunction in mitral valve prolapse: a quantitative dynamic 3D echocardiographic study, JACC Cardiovasc. Imaging 10 (12) (2017) 1424–1433.

[4] M. Perazzolo Marra, C. Basso, M. De Lazzari, S. Rizzo, A. Cipriani, B. Giorgi, C. Lacognata, I. Rigato, F. Migliore, K. Pilichou, L. Cacciavillani, E. Bertaglia, A. C. Frigo, B. Bauce, D. Corrado, G. Thiene, S. Iliceto, Morphofunctional abnormalities of mitral annulus and arrhythmic mitral valve prolapse, Circ. Cardiovasc. Imaging 9 (8) (2016), e005030.

[5] P. Carmo, M.J. Andrade, C. Aguiar, R. Rodrigues, R. Gouveia, J.A. Silva, Mitral annular disjunction in myxomatous mitral valve disease: a relevant abnormality recognizable by transthoracic echocardiography, Cardiovasc. Ultrasound 8 (2010) 53.

[6] M.J. Eriksson, C.Y. Bitkover, A.S. Omran, T.E. David, J. Ivanov, M.J. Ali, A. Woo, S. C. Siu, H. Rakowski, Mitral annular disjunction in advanced myxomatous mitral valve disease: echocardiographic detection and surgical correction, J. Am. Soc. Echocardiogr. 18 (10) (2005) 1014–1022.

[7] L.A. Dejgaard, E.T. Skjolsvik, O.H. Lie, M. Ribe, M.K. Stokke, F. Hegbom, E. S. Scheirlynck, E. Gjertsen, K. Andresen, T.M. Helle-Valle, E. Hopp, T. Edvardsen, K.H. Haugaa, The mitral annulus disjunction arrhythmic syndrome, J. Am. Coll. Cardiol. 72 (14) (2018) 1600–1609.

[8] M. Chivulescu, K. Krohg-Sorensen, E. Scheirlynck, B.R. Lindberg, L.A. Dejgaard, O. H. Lie, T. Helle-Valle, E.T. Skjolsvik, M.E. Estensen, T. Edvardsen, P.S. Lingaas, K. H. Haugaa, Mitral annulus disjunction is associated with adverse outcome in Marfan and Loeys-Dietz syndromes, Eur. Heart J. Cardiovasc. Imaging (2020).

[9] T. Konda, T. Tani, N. Suganuma, H. Nakamura, T. Sumida, Y. Fujii, J. Kawai, T. Kitai, K. Kim, S. Kaji, Y. Furukawa, The analysis of mitral annular disjunction detected by echocardiography and comparison with previously reported pathological data, J. Echocardiogr. 15 (4) (2017) 176–185.

[10] P. Blanke, J.R. Weir-McCall, S. Achenbach, V. Delgado, J. Hausleiter, H. Jilaihawi, M. Marwan, B.L. Norgaard, N. Piazza, P. Schoenhagen, J.A. Leipsic, Computed tomography imaging in the context of transcatheter aortic valve implantation (TAVI) / transcatheter aortic valve replacement (TAVR): An expert consensus document of the Society of Cardiovascular Computed Tomography, J. Cardiovasc. Comput. Tomogr. 13 (1) (2019) 1–20.

[11] R. Hinzpeter, M. Eberhard, P. Burghard, F.C. Tanner, M. Taramasso, R. Manka, G. Feuchtner, F. Maisano, H. Alkadhi, Computed tomography in patients with tricuspid regurgitation prior to transcatheter valve repair: dynamic analysis of the annulus with an individually tailored contrast media protocol, EuroIntervention 12 (15) (2017) e1828–e1836.

[12] M. Francone, R.P.J. Budde, J. Bremerich, J.N. Dacher, C. Loewe, F. Wolf, L. Natale, G. Pontone, A. Redheuil, R. Vliegenthart, K. Nikolaou, M. Gutberlet, R. Salgado, CT and MR imaging prior to transcatheter aortic valve implantation: standardisation of scanning protocols, measurements and reporting-a consensus document by the European Society of Cardiovascular Radiology (ESCR), Eur. Radiol. 30 (5) (2020) 2627–2650.

[13] A. Gupta, E.G. Kikano, K. Bera, D. Baruah, S.S. Saboo, S. Lennartz, N.G. Hokamp, A. Gholamrezanezhad, R.C. Gilkeson, K.R. Laukamp, Dual energy imaging in cardiothoracic pathologies: a primer for radiologists and clinicians, Eur. J. Radiol. Open 8 (2021).

[14] P. Blanke, D. Dvir, A. Cheung, J. Ye, R.A. Levine, B. Precious, A. Berger, D. Stub, C. Hague, D. Murphy, C. Thompson, B. Munt, R. Moss, R. Boone, D. Wood, G. Pache, J. Webb, J. Leipsic, A simplified D-shaped model of the mitral annulus to facilitate CT-based sizing before transcatheter mitral valve implantation, J. Cardiovasc. Comput. Tomogr. 8 (6) (2014) 459–467.

[15] H. Alkadhi, L. Desbiolles, P. Stolzmann, S. Leschka, H. Scheffel, A. Plass, T. Schertler, P.T. Trindade, M. Genoni, P. Cattin, B. Marincek, T. Frauenfelder, Mitral annular shape, size, and motion in normals and in patients with cardiomyopathy: evaluation with computed tomography, Invest. Radiol. 44 (4) (2009) 218–225.

[16] G.M. Feuchtner, H. Alkadhi, C. Karlo, A. Sarwar, A. Meier, W. Dichtl, S. Leschka, R. Blankstein, J. Gruenenfelder, P. Stolzmann, R.C. Cury, Cardiac CT angiography for the diagnosis of mitral valve prolapse: comparison with echocardiography1, Radiology 254 (2) (2010) 374–383.

[17] L. Faggioni, M. Gabelloni, S. Accogli, M. Angelillis, G. Costa, P. Spontoni, A. S. Petronio, D. Caramella, Preprocedural planning of transcatheter mitral valve interventions by multidetector CT: what the radiologist needs to know, Eur. J. Radiol. Open 5 (2018) 131–140.

[18] M. Eberhard, A.L.N. Schonenberger, R. Hinzpeter, A. Euler, J. Sokolska, L. Weber, N. Kuzo, R. Manka, A.M. Kasel, F.C. Tanner, H. Alkadhi, Mitral annular calcification in the elderly - Quantitative assessment, J. Cardiovasc. Comput. Tomogr. (2020).

[19] T. Okuno, M. Asami, F. Khan, F. Praz, D. Heg, J. Lanz, M. Kassar, O.K. Khalique, C. Grani, N. Brugger, L. Raber, S. Stortecky, M. Valgimigli, S. Windecker, T. Pilgrim, Does isolated mitral annular calcification in the absence of mitral valve disease affect clinical outcomes after transcatheter aortic valve replacement? Eur. Heart J. Cardiovasc. Imaging 21 (5) (2020) 522–532.

[20] A.P. Kappetein, S.J. Head, P. Genereux, N. Piazza, N.M. van Mieghem, E. H. Blackstone, T.G. Brott, D.J. Cohen, D.E. Cutlip, G.A. van Es, R.T. Hahn, A. J. Kirtane, M.W. Krucoff, S. Kodali, M.J. Mack, R. Mehran, J. Rodes-Cabau, P. Vranckx, J.G. Webb, S. Windecker, P.W. Serruys, M.B. Leon, Updated standardized endpoint definitions for transcatheter aortic valve implantation: the Valve Academic Research Consortium-2 consensus document, Eur. Heart J. 33 (19) (2012) 2403–2418.

[21] M. Eberhard, G. Milanese, M. Ho, S. Zimmermann, T. Frauenfelder, F. Nietlispach, F. Maisano, F.C. Tanner, T.D.L. Nguyen-Kim, Pre-procedural CT angiography inferior vena cava measurements: a predictor of mortality in patients undergoing transcatheter aortic valve implantation, Eur. Radiol. 29 (2) (2019) 975–984.

[22] K. Higashigaito, T. Schmid, G. Puippe, F. Morsbach, M. Lachat, B. Seifert, T. Pfammatter, H. Alkadhi, D.B. Husarik, CT angiography of the aorta: prospective evaluation of individualized low-volume contrast media protocols, Radiology 280 (3) (2016) 960–968.

[23] T. Jurencak, J. Turek, B.L. Kietselaer, C. Mihl, M. Kok, V.G. van Ommen, L.A. van Garsse, E.C. Nijssen, J.E. Wildberger, M. Das, MDCT evaluation of aortic root and aortic valve prior to TAVI. What is the optimal imaging time point in the cardiac cycle? Eur. Radiol. 25 (7) (2015) 1975–1983.

[24] A.J. Putnam, K. Kebed, V. Mor-Avi, N. Rashedi, D. Sun, B. Patel, H. Balkhy, R. M. Lang, A.R. Patel, Prevalence of mitral annular disjunction in patients with mitral valve prolapse and severe regurgitation, Int. J. Cardiovasc. Imaging 36 (7) (2020) 1363–1370.

[25] R. Hinzpeter, M. Eberhard, A. Pozzoli, J. von Spiczak, R. Manka, F.C. Tanner, M. Taramasso, F. Maisano, H. Alkadhi, Dynamic anatomic relationship of the coronary arteries to the valves. Part 1: mitral annulus and circumflex artery, EuroIntervention 15 (10) (2019) 919–922.

[26] I.J. Amat-Santos, A. Revilla, J. Lopez, C. Cortes, H. Gutierrez, A. Serrador, F. Gimeno, A. Puerto, I. Gomez, J.A. San Roman, Value of CT in patients undergoing self-expandable TAVR to assess outcomes of concomitant mitral regurgitation, JACC Cardiovasc. Imaging 8 (2) (2015) 226–227.

[27] P. Lancellotti, C. Tribouilloy, A. Hagendorff, B.A. Popescu, T. Edvardsen, L. A. Pierard, L. Badano, J.L. Zamorano, I. Scientific Document Committee of the European Association of Cardiovascular, Recommendations for the echocardiographic assessment of native valvular regurgitation: an executive summary from the European Association of Cardiovascular Imaging, Eur. Heart J. Cardiovasc. Imaging 14 (7) (2013) 611–644.

[28] H. Baumgartner, V. Falk, J.J. Bax, M. De Bonis, C. Hamm, P.J. Holm, B. Iung, P. Lancellotti, E. Lansac, D. Rodriguez Munoz, R. Rosenhek, J. Sjogren, P. Tornos Mas, A. Vahanian, T. Walther, O. Wendler, S. Windecker, J.L. Zamorano, E.S.C.S.D. Group, ESC/EACTS Guidelines for the management of valvular heart disease, Eur. Heart J. 38 (36) (2017) 2739–2791 (2017).

[29] W.A. Zoghbi, D. Adams, R.O. Bonow, M. Enriquez-Sarano, E. Foster, P.A. Grayburn, R.T. Hahn, Y. Han, J. Hung, R.M. Lang, S.H. Little, D.J. Shah, S. Shernan, P. Thavendiranathan, J.D. Thomas, N.J. Weissman, Recommendations for noninvasive evaluation of native valvular regurgitation: a report from the american society of echocardiography developed in collaboration with the society for cardiovascular magnetic resonance, J. Am. Soc. Echocardiogr. 30 (4) (2017) 303–371.

[30] B. Essayagh, L. Iacuzio, F. Civaia, J.F. Avierinos, C. Tribouilloy, F. Levy, Usefulness of 3-Tesla cardiac magnetic resonance to detect mitral annular disjunction in patients with mitral valve prolapse, Am. J. Cardiol. 124 (11) (2019) 1725–1730.

[31] G.C.M. Siontis, F. Praz, J. Lanz, R. Vollenbroich, L. Roten, S. Stortecky, L. Raber, S. Windecker, T. Pilgrim, New-onset arrhythmias following transcatheter aortic valve implantation: a systematic review and meta-analysis, Heart 104 (14) (2018) 1208–1215.

[32] T.H. Jorgensen, H.G. Thyregod, J.B. Tarp, J.H. Svendsen, L. Sondergaard, Temporal changes of new-onset atrial fibrillation in patients randomized to surgical or transcatheter aortic valve replacement, Int. J. Cardiol. 234 (2017) 16–21.

[33] B.E. Stahli, M. Reinthaler, D.M. Leistner, U. Landmesser, A. Lauten, Transcatheter aortic valve replacement and concomitant mitral regurgitation, Front. Cardiovasc. Med. 5 (2018) 74.